The Crystal Structure of Valentinite (Orthorhombic Sb_2O_3)[1].

By **M. J. Buerger** and **Sterling B. Hendricks**,
Mineralogical Laboratory, Massachusetts Institute of Technology, Cambridge, Massachusetts, U.S.A., and Bureau of Chemistry and Soils, United States Department of Agriculture, Washington, D.C., U.S.A.

Table of Contents.

Abstract.

Natural valentinite from Su Suergiu, Sardinia, and also artificial valentinite made by subliming chemically pure Sb_2O_3 above its inversion point, have been studied by the Weißenberg method. The structure has been completely and uniquely determined.

The three symmetry planes indicated by Weißenberg symmetry study confirm the orthorhombic character of this crystal. These all prove to be glide planes, which permits a unique determination of the space group. An intensive intensity study has been made resulting in a unique determination of the correct antimony equipoint combination and all antimony parameters, and a unique determination of the oxygen equipoint combination and oxygen x and y parameters. The only parameters remaining undetermined by direct intensity deduction are the two which fix the elevations of the two kinds of oxygen atoms. In order to avoid an unduly lengthy

1) The structure was worked out independently by the two authors, who derived identical symmetry information, substantially identical cell dimensions, and also closely the same parameter values. When this duplication of effort was discovered, joint publication was agreed upon. The methods and arguments given in this paper are essentially those used by Buerger.

investigation, these last parameters were tentatively fixed by simple physical considerations. A slight permissible adjustment of these predicted values yielded perfect agreement between observed and calculated intensities.

The valentinite structure and some of its characteristics may be described in the following terms:

Diffraction symbol:	$mmmPccn$
Crystal class	$mmm = D_{2h}$
Space group	$Pccn = D_{2h}^{10}$
Unit cell	$a = 4.92$ Å
	$b = 12.46$
	$c = 5.42$
	$Z = 4Sb_2O_3$ per cell

Equipoints and parameters:

	x	y	z	u
$8Sb$ in $8e$ with	$.044_4$	$.128_3$	.179	
$4O_{\mathrm{I}}$ in $4c$ with				.029
$8O_{\mathrm{II}}$ in $8e$ with	.147	.058	—.139	

The structure is composed of strings of

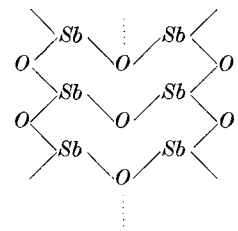

extending along one set of two-fold rotation axes. The Sb—O distances within a string are about 2.00 Å, which is in good agreement with the electron-pair bond distance. The strings pack together across symmetry centers in such a way that the antimonys of one chain come about opposite the oxygens of the neighboring chain and are held apart by O—O contacts of 2.54 Å separation. This structure of indefinitely long chain molecules accounts well for the perfect prismatic cleavage of the crystal.

Data are presented for the construction of a model illustrating the structure.

Introduction.

Sb_2O_3 is dimorphous. According to sublimation experiments by Roberts and Fenwick[1]) the cubic form, senarmontite, is stable below 570° C. while the orthorhombic form, valentinite, is stable above this temperature. Confirmation of this in a general way has been provided

1) Roberts, E. J., and Fenwick, F., The antimony-antimony trioxide electrode and its use as a measure of acidity: J. Amer. Chem. Soc. **50** (1928) esp. 2134.

in measurements of the vapor pressures of the two forms by Hincke[1]). The crystal structure of the cubic modification has been determined by Bozorth[2]). No information regarding the structure of the orthorhombic form has hitherto been published.

Material.

A complete investigation was carried out (by Buerger) using natural valentinite from Su Suergiu, Sardinia. Crystals from this source have been crystallographically described by Millosevich[3]). This valentinite is in the form of small, more or less equidimensional crystals, each consisting of a very short prism of height about equal to width, surmounted by rounded termini. Good goniometric measurements, unfortunately, are impossible on this material due to an extreme tendency to lineage. The cleavage prism angle is in the general region of 42° 18′, corresponding to an axial ratio .3869 : 1, but this can not be duplicated.

A complete investigation was also carried out (by Buerger) on valentinite grown by sublimation from pure Sb_2O_3 in an atmosphere of nitrogen. This material was kindly prepared by Mr. M. C. Bloom of the Mineralogical Laboratory, Massachusetts Institute of Technology. The crystals of sublimed valentinite used are very flat prismatic in habit, consisting essentially of unit prism and blunt pyramid terminus. The prism, which is highly striated, has a interfacial angle of approximately 43° 17′, corresponding to an axial ratio $a : b = .3967 : 1$, but very considerable variations from these values were observed.

An independent analysis (by Hendricks) was carried out on natural valentinite from an unknown Sardinian locality and on crystals obtained from a vug in pure Sb_2O_3 that had been melted in an atmosphere of nitrogen. The natural valentinite, which was kindly supplied by Dr. W. F. Foshag, was a portion of specimen No. R 1742 from the collection of the National Museum. Crystals were pyramidal in habit showing predominant development of (110) with many other forms. All of the natural crystals were multiple. The artificial crystals were similar in habit to those described above.

1) Hincke, W. B., The vapor pressure of antimony trioxyde, J. Amer. Chem. Soc. **52** (1930) 3869.

2) Bozorth, Richard M., The crystal structures of the cubic forms of arsenious and antimonous oxides, J. Amer. Chem. Soc. **45** (1923) 1621.

3) Millosevich, Federico, Appunti di Mineralogia Sarda — 2° Valentinite della miniera de antimonio di Su Suergiu (Gerrei), Atti Accad. Lincei **9** (5) (1900) 340.

Space Pattern Characteristics.

Method. The entire investigation was carried out using the equi-inclination[1,2] Weissenberg method. Crystal fragments of the order of half a millimeter in diameter were completely bathed in unfiltered beams of copper radiation for the purpose of determining the cell characteristics. Molybdenum radiation was also employed for the purpose of recording high order reflections necessary in the determination of parameters.

The general methods of interpreting equi-inclination photographs have been discussed elsewhere[1,2]. These have been applied as indicated beyond.

Table I.

Possible Ways of Accomodating 8 *Sb* and 12 *O* in *Pccn* (D_{2h}^{10}).

8 *Sb* in	12 *O* in
(1) $4_a + 4_b$	(1) $4_a + 4_b + 4_c$
(2) $4_a + 4_c$	(2) $4_a + 4_b + 4_d$
(3) $4_a + 4_d$	(3) $4_a + 4_c + 4_c$
(4) $4_b + 4_c$	(4) $4_a + 4_c + 4_d$
(5) $4_b + 4_d$	(5) $4_a + 4_d + 4_d$
(6) $4_c + 4_c$	(6) $4_b + 4_c + 4_c$
(7) $4_c + 4_d$	(7) $4_b + 4_c + 4_d$
(8) $4_d + 4_d$	(8) $4_b + 4_d + 4_d$
(9) 8_e	(9) $8_e + 4_a$
	(10) $8_e + 4_b$
	(11) $8_e + 4_c$
	(12) $8_e + 4_d$

Photographs. Zero level photographs were taken for rotations about the three crystallographic axes of both natural and pure, sublimed material. First layer photographs were taken about the *a* axis of a natural crystal (Hendricks); first, second, third and fourth layer photographs were taken for *b* axis rotations of the natural Su Suergiu material (Buerger). First, second and third layer photographs were also taken for the *c* axis rotation of the sublimed material (Buerger).

Centrosymmetrical point-group. The photographs of all levels investigated for each of the three crystallographic axial rotations of both natural and sublimed valentinite agree in assigning the symmetry C_{2l} to the reciprocal lattice levels represented by the photographs.

1) Buerger, M. J., The Weißenberg reciprocal lattice projection and the technique of interpretating Weißenberg photographs, Z. Kristallogr. (A) **88** (1934) 356.

2) Buerger, M. J., The application of plane groups to the interpretation of Weißenberg photographs, Z. Kristallogr. (A) **91** (1935) 255.

Space group. By comparison with the reciprocal translations given by the n-layer photographs discussed above and with the layer line spacing of the rotation photograph of corresponding axial rotation, the reciprocal translations on the three axial zero-layer photographs appear to be doubled as follows:

crystal rotation axis	doubled translation on zero-level of reciprocal lattice
a	t_c
b	t_c
c	$t_a + t_b$

This indicates three glide planes: ccn. The diffraction symbol is therefore $mmmPccn$. The presence of the three mutually orthogonal glide planes definitely establishes the holohedral orthorhombic symmetry, $mmm = D_{2h}$, of valentinite and definitely establishes the space group as $Pccn = D_{2h}^{10}$.

Unit cell. The dimensions of the unit cell were determined by direct film measurements from the b-axis layer spacing and from the Z-spacing of the pattern along symmetry lines for the b-axis n-layers. These measurements were subsequently refined by direct steel scale measurements of x of high-order reflections on the three zero-layer photographs with the aid of the relation:

$$d = \frac{n}{2 \sin\left(\frac{x}{2} \cdot \frac{360}{2\pi r_F}\right)}$$

The dimensions of cells of the natural Su Suergiu material and of the chemically pure sublimed Sb_2O_3 are substantially the same:

	absolute	ratio	Axial Ratios obtained from Surface Morphological study	
			Millosevich's Su Suergiu[1])	Goldschmidt's average[2])
a	4.92 Å	.395	.39122	.3936
b	12.46	1.	1.	1.
c	5.42	.435	—	4339

Lattice dimensions obtained from layer photographs and high order reflections from the pinacoids on equatorial zone Weissenberg photographs (by Hendricks) on the natural material are $a = 4.91$ Å,

1) Millosevich, Federico, Appunti di Mineralogia Sarda — 2° Valentinite della miniera de antimonio di Su Suergiu (Gerrei), Atti Accad. Lincei **9** (5) (1900) 340.

2) Goldschmidt, Victor, Atlas der Kristallformen **9** (1923) 45.

$b = 12.47$ Å, $c = 5.41$ Å. Values for the artificial crystals agreed closely with these. Angles measured on Weissenberg photographs and calculated values according to these lattice dimensions are:

Angle	Measured	Calculated
$110 : 1\bar{1}0$	42° 48′	43° 00′
$011 : 0\bar{1}1$	46° 48′	46° 50′

The axial ratio chosen from surface morphological study is thus based upon the correct structural cell.

Using Spencer's value[1]) of 5.76 for the density of natural valentinite, these cell dimensions require 4.006 formula weights of Sb_2O_3 per unit cell of the Su Suergiu material.

Possible Structures.

Space group D_{2h}^{10} has the following equipoints:

rank	location	designation
Four-fold positions	symmetry centers	4_a
	symmetry centers	4_b
	two-fold axes	4_c
	two-fold axes	4_d
Eight-fold position	general	8_e

Four formula weights of Sb_2O_3, or 8 *Sb* and 12 *O*, must be accomodated by these equipoints. The possible ways in which this accomodation can be effected are listed in table I. Not all combinations of these positions, however, are possible. Because of the absence of degrees of freedom in 4_a and 4_b, only one of each of these may appear in the entire combination.

Reflection Intensities.

The amplitude of the waves scattered by the atoms occupying the general 8-fold equipoint is given by the expressions of table II for the various cases of h, k, and l, the indices of the reflection. The reflection vanishes for conditions not included in the table.

For comparison of observed with calculated intensities, the former were visually estimated from Weissenberg equatorial films taken chiefly with *Mo*-K_α and *Mo*-K_β radiation. Comparisons between the stronger reflection intensities were derived from underexposed films and comparisons between the weaker reflections were derived from films made

1) Spencer, L. J., Notes on some Bolivian minerals (jamesonite, andorite, cassiterite, tourmaline, &c.), Mineral. Mag. 14 (1907) 331.

with extremely long exposures. The intensities of the spectra for these conditions have been calculated by means of the relation

$$\sqrt{I} = \sqrt{\frac{1 + \cos^2 2\theta}{2 \sin 2\theta}} A$$

where I = the intensity
A = the appropriate structure amplitude
θ = the Bragg glancing angle

Location of Antimony Atoms.

Elimination of incorrect antimony equipoint combinations. Certain possible combinations of antimony equipoints listed in

Table III.

Regularities in structural amplitude series for even orders of pinacoid reflections.

Sb equipoint combination	(100)	(010)	(001)
$4_a + 4_b$	F (8, 8, 8, 8———)	F (8, 8, 8, 8———)	F (8, 8, 8, 8———)
$4_a + 4_c$	F (8, 0, 8, 0———)	F (8, 0, 8, 0———)	irregular
$4_a + 4_d$	F (8, 0, 8, 0———)	F (8, 0, 8, 0———)	irregular
$4_b + 4_c$	F (8, 0, 8, 0———)	F (8, 0, 8, 0———)	irregular
$4_b + 4_d$	F (8, 0, 8, 0———)	F (8, 0, 8, 0———)	irregular
$4_c + 4_c$	F (−8, 8, −8, 8——)	F (−8, 8, −8, 8——)	irregular
$4_c + 4_d$	F (−8, 8, −8, 8——)	F (−8, 8, −8, 8——)	irregular
$4_d + 4_d$	F (−8, 8, −8, 8——)	F (−8, 8, −8, 8——)	irregular
$8e$	irregular	irregular	irregular

Note: designation irregular indicates that the series does not necessarily contain regularities, although it may show regularity with certain parameter values.

table I can be easily eliminated by very simple intensity considerations: For the present purpose it is sufficient to compare observed pinacoid reflection intensities with those to be expected with the antimony atoms occupying the several possible equipoint combinations. The expected intensities can be approximated closely enough for the purpose by means of the structure amplitudes of the antimony atoms alone. These are listed in table III. The actual intensities must follow the essential features of the several series listed in this table because of the relatively great scattering power of the antimony atom compared with that of the oxygen atom. The actual location of the oxygen atoms can effect the intensities indicated, at most, by giving rise to weak reflections where the structure amplitudes of table IV indicate an absent reflection, *O*,

and by very slightly disturbing the relative intensities involved in regular declines indicated by the designation F (8).

Table III indicates that regular intensity declines for the even order reflections of the 100 and 010 series, either with or without alternate absences, characterize all structures containing antimony occupying the special equipoints. The actual photographs display an intensity

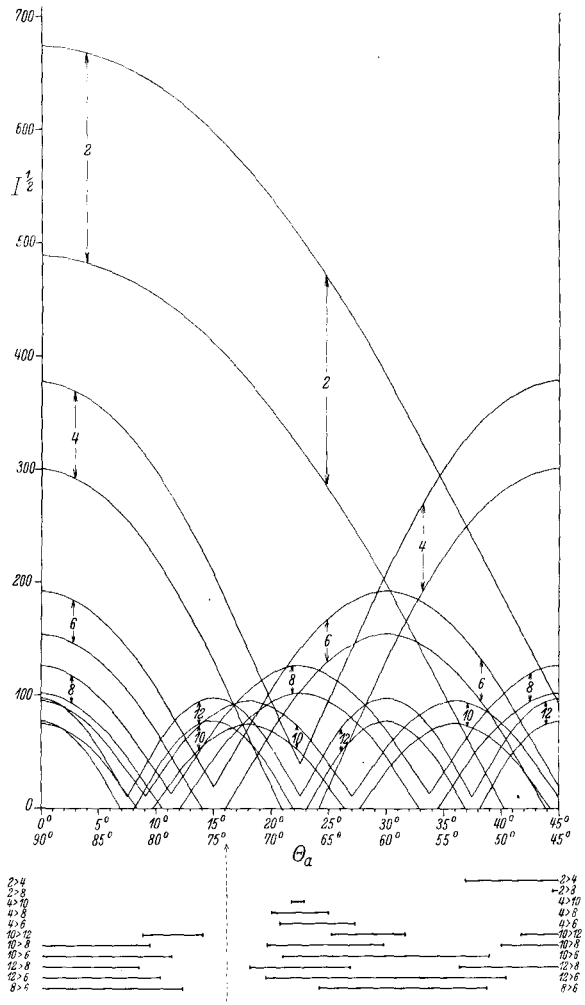

Fig. 1. Variations of intensity of the orders of 100 (Mo-K_α radiation) with the antimony parameter, θ_a, and parameter regions eliminated by observed intensity relations. The half-widths of the bands represent the intensity uncertainties due to the initial uncertainty in the positions of the oxygen atoms.

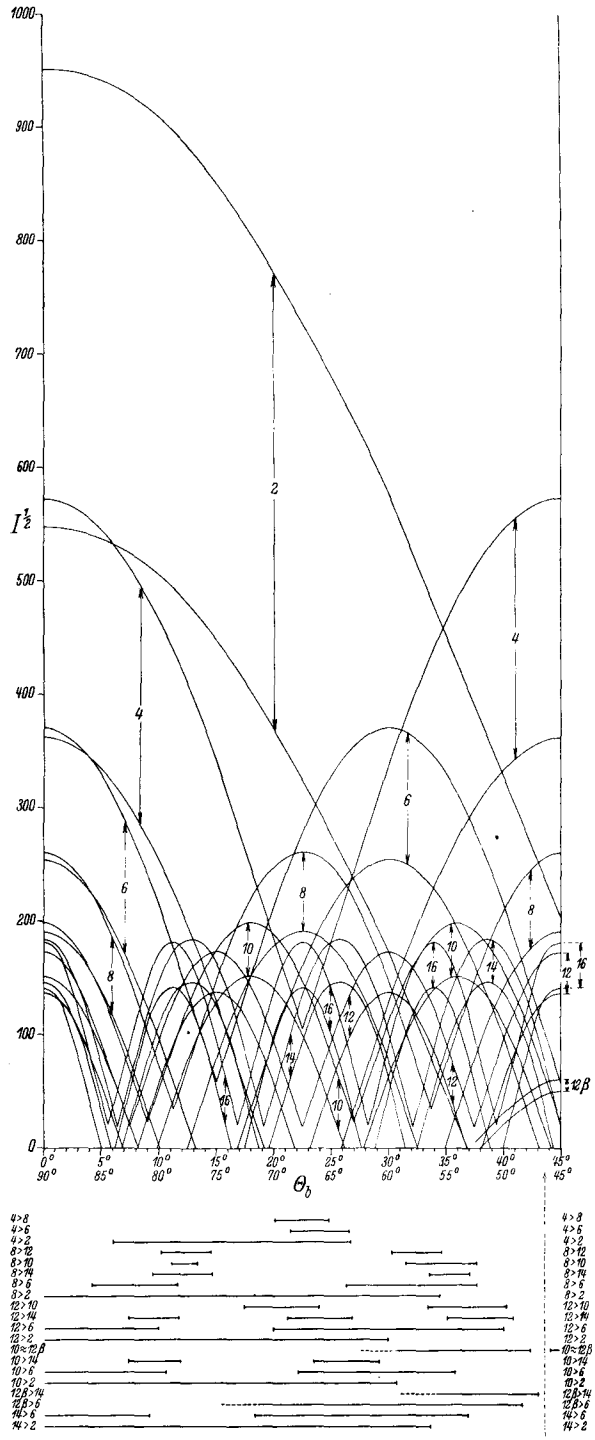

Fig. 2. Variations of intensity of the orders of 010 (Cu-$K_{\alpha+\beta}$ radiation) with the antimony parameter, θ_b, and parameter regions eliminated by observed intensity relations. The half-widths of the bands represent the intensity uncertainties due to the initial uncertainty in the positions of the oxygen atoms.

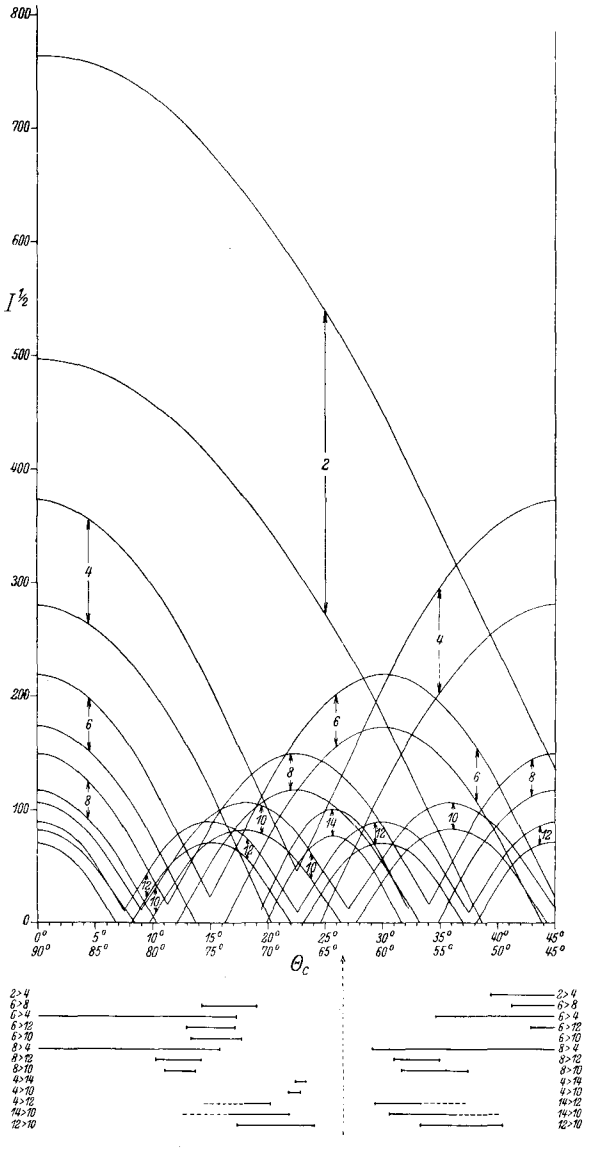

Fig. 3.

Variations of intensity of the orders of 001 (Mo-K_α radiation) with the antimony parameter, θ_c, and parameter regions eliminated by observed intensity relations. The half-widths of the bands represent the intensity uncertainties due to the initial uncertainty in the positions of the oxygen atoms.

series comparable with one of these regularities namely, regular decline with alternate absences, but only for one pinacoid reflection series, 010; other series are distinctly irregular. The antimony atoms can accordingly occupy only the general 8-fold position. The meaning of the regular decline of even order reflections from (010) with alternate absences is obviously that the antimony atoms are arranged in sheets parallel to (010) which are spaced approximately one quarter of the b identity period apart. This would give an antimony y parameter of approximately $\frac{1}{8}$.

Antimony parameters. Antimony has such a large atomic number, 51, compared with oxygen, 8, that the scattering power of the antimony dominates the character of the spectra. It is therefore possible to very approximately locate the parameters of the single set of antimony atoms in the general position irrespective of the position of the oxygen atoms. The determination of these parameters is shown graphically in Figs. 1, 2, and 3. In these diagrams the square roots of the intensities of the observable orders of pinacoid reflections are plotted against θ_a, θ_b and θ_c, the angular parameters along the a, b, and c crystallographic axes. The antimony contributions to the intensities impart the general appearances to the intensity variations with parameter, and the oxygen contributions, being unknown at this stage of the investigation, are given their widest possible values. Instead of the usual cosine curves representing the variation of amplitude with position, therefore, the figures show bands whose centers are these cosine curves, and whose widths cover the intensity uncertainties in both directions due to the preliminary lack of knowledge of the oxygen positions.

Because of the great length of the b axis, 12.46 Å, it is possible to record 34 orders of reflection from (010) with $Mo\text{-}K_\alpha$ radiation. It is therefore possible to refine the y parameter of antimony to a very accurate value, irrespective of the positions of the oxygen atoms. This is carried out graphically in figure 4.

Since the space group provides for halved spacings of all the pinacoid sheets, only even orders of pinacoid reflections appear. This absence of odd order reflections gives rise to two solutions for each parameter value. With the eliminations shown in figures 1, 2, 3, and 4, these approximate solutions are:

$$\theta_a = 16^\circ \text{ and } 74^\circ, \quad \theta_b = 43.8^\circ \text{ and } 46.2^\circ, \quad \theta_c = 26\tfrac{1}{2}^\circ \text{ and } 63\tfrac{1}{2}^\circ.$$

The incorrect value of each of these pairs may be eliminated by a consideration of more general spectra involving odd values of h, k, and l, respectively.

The structure factor for $hk0$ reflections for odd values of h is $-8 \sin h\theta_a \sin k\theta_b$. When h is 5, this is a maximum at 18° and zero at 72°. Since the spectral series $5k0$ forms one of the strongest festoons on the Weissenberg c axis equator photograph, it may be safely concluded that the correct value of θ_a is approximately 16°, not 74°.

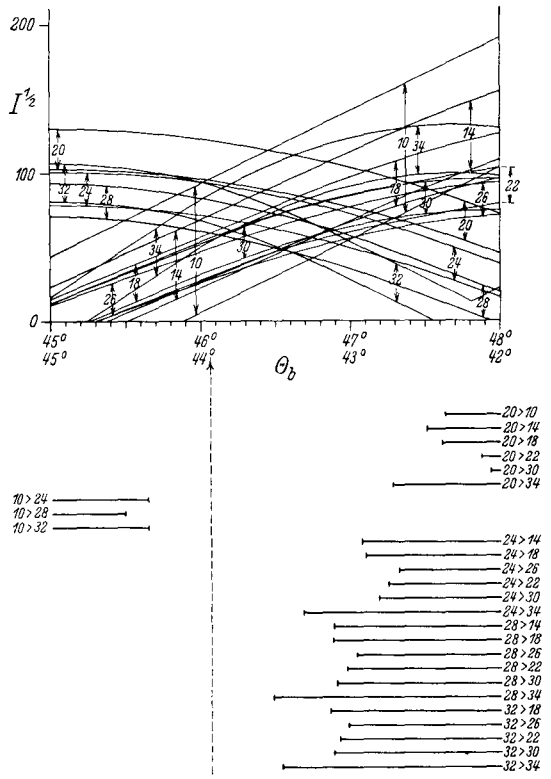

Fig. 4. Variations of intensity of the higher orders of 010 (Mo-K_α radiation) with the antimony parameter, θ_b, and parameter regions eliminated by observed intensity relations. The half-widths of the bands represent the intensity uncertainties due to the initial uncertainty in the positions of the oxygen atoms.

To eliminate the incorrect value of θ_b, the structure factor may be applied to $h \cdot 29.0$ and $h \cdot 31.0$. For these we have:

at 43.8° $\begin{cases} \sin(29 \times 43.8°) = \sin 1270° = \sin(-190°): \text{almost zero.} \\ \sin(31 \times 43.8°) = \sin 1358° = \sin(-82°): \text{almost a maximum.} \end{cases}$

at 46.2° $\begin{cases} \sin(29 \times 46.2°) = \sin 1340° = \sin(-90°): \text{almost a maximum.} \\ \sin(31 \times 46.2°) = \sin 1432° = \sin(-8°): \text{almost zero.} \end{cases}$

The series $h \cdot 29.0$ is strong and the series $h \cdot 31.0$ is absent on the Weissenberg c axis equator film. The correct value of the θ_b is accordingly near 46.2°.

Unfortunately the elimination of the incorrect values of the θ_c parameter cannot be made in a similar manner from $h0l$ and $0kl$ spectra because the (100) and (010) glide planes, both with components $c/2$, extinguish these spectra when l is odd. Recourse may be had to the general reflections, however, using the same methods. The two possible regions lie near 30° and 60°. For these regions $hk3$ reflections give important information because

$$\begin{aligned} \cos\ (3 \times 30°) &= \cos\ 90° = 0 \\ \sin\ (3 \times 30°) &= \sin\ 90° = \text{a maximum.} \\ \cos\ (3 \times 60°) &= \cos\ 180° = \text{a maximum.} \\ \sin\ (3 \times 60°) &= \sin\ 180° = 0. \end{aligned}$$

A general survey of $hk3$ spectra shows that those referable to structure factors involving $\cos l\theta_c$ are usually strong, while those referable to structure factors involving $\sin l\theta_c$ are either weak or absent. This definitely places θ_c in the region of 60° rather than 30°, and retains $63\frac{1}{2}°$ as the correct alternative.

The correct approximate antimony parameters may now be tabulated:

$\theta_a = 16°$	$x = .044_4$
$\theta_b = 46.2°$	$y = .128_3$
$\theta_c = 63\frac{1}{2}°$	$z = .176_4$

A slight refinement of the x and z values will be made after the oxygen atoms are located.

Location of Oxygen Atoms.

Method of location. The antimony atoms were located, as already discussed, with the aid of the intensity bands illustrated in Figs. 1—4. For all the information taken into account, the calculated and observed intensities are in complete harmony for the antimony parameters listed in the last section. There are, however, other intensity features which have not as yet been considered, and which depend upon the location of the oxygen atoms. These will now receive consideration.

The plan of attack in the location of the oxygen positions is as follows: First of all, the y positions of the antimony atoms can be located with great precision because so many orders of 010 are available (17 even orders, from 2 to 34). The band width, of course, as already explained,

is the intensity uncertainty due to the unknown oxygen positions. In order to have the calculated intensities of the 010 spectra arranged in the observed relative order, the calculated intensities must be within certain very definite regions of the oxygen uncertainty bands. In other words, the phase sign, and even an estimate of the absolute value of the oxygen contribution may be obtained for some spectra, especially where the maximum possible oxygen contribution is large, as in reflections of low sin θ value.

Certain equipoint combinations can be discarded on the grounds that they could not furnish the required oxygen contributions, and the y parameters of the correct oxygen equipoint combination may be determined independently of every other variable except the antimony y parameter, which, as already mentioned, is very certainly and accurately established.

With the antimony x and y parameters known, and oxygen equipoints and y parameters established, the oxygen x parameters may be determined by a study of the relative intensities of the $hk0$ spectra. Many comparisons, such as 800 with 840, 10.0.0 with 10.4.0, 12.0.0 with 12.4.0 etc., may be made which are almost independent of the antimony parameters, so the small uncertainty of the antimony position in the x direction is no bar to the accurate determination of the x oxygen parameters. Definite phase and amplitude requirements within the oxygen uncertainty bands then locate the oxygen atoms quite accurately.

At this stage, the projection of the valentinite structure on (001) becomes accurately established and the rough structural plan is fairly obvious. Only few trial calculations need be made in physically possible oxygen z positions for the correct structure.

Elimination of certain incorrect oxygen equipoint combinations and determination of oxygen y parameters. The antimony y parameter may be taken, from Figs. 2 and 1 as $\theta_b = 46.2°$, $y = .128_3$, with very little uncertainty. Referring, now, to the photographs taken with copper radiation, it is striking that 020 and 060, which have a considerable possible oxygen contribution, are absent and exceedingly weak respectively. The absolute values of the amplitudes of these two reflections must, therefore, be approximately zero. The oxygen amplitude contributions to give this net value of zero at antimony $\theta_b = 46.2°$ must be about + 30 for 020 and — 38 for 060. The further relationships $0.10.0 = 0.12.0\,\beta \geqq 0.14.0$ give the added requirements that the oxygen amplitude contribution to 0.10.0 be negative and

Table IV.

Intensity condition	Oxygen contribution to amplitude of reflection, required at $Sb\theta_b = 46.2°$	
020 absent	020	+ 30
060 very faint	060	− 38
$0.10.0 = 0.12.0\ \beta$	0.10.0	− 16 (−) maximum
$0.14.0 \leqq 0.12.0\ \beta$	0.14.0	≈ 0

rather extreme, and to 0.14.0, approximately zero. These conditions are summarized in Table IV.

The oxygen atoms may be in any of the 8 equipoint combinations listed in Table I. The contribution of the oxygens to the $0k0$ reflections for the several equipoints reduces as follows:

$$8_e \quad , \quad \left|\sqrt{\frac{1+\cos^2 2\theta}{2\sin 2\theta}}\cdot 8F_0 \cos\theta_b\right|$$

$$4a \text{ or } 4b, \quad \sqrt{\frac{1+\cos^2 2\theta}{2\sin 2\theta}}\cdot 4F_0$$

$$4c \text{ or } 4d, \pm\sqrt{\frac{1+\cos^2 2\theta}{2\sin 2\theta}}\cdot 4F_0$$

Combinations of the several special positions, (1) — (8), give only invariable net amplitudes of

$$\pm\sqrt{\frac{1+\cos^2 2\theta}{2\sin 2\theta}}\cdot \begin{Bmatrix} 12 \\ 8 \\ 4 \end{Bmatrix} F_0$$

none of which have the possibility of making the oxygen amplitude contribution to 020 equal to + 30. Hence all special position equipoint combinations, (1)—(8) are eliminated.

The other equipoint combinations, (9)—(12), contain the variable, $\cos\theta_b$, and hence give more variable reflection possibilities. The variation of oxygen amplitude contribution with θ_b for combinations (9), $8_e + 4_a$, and (10), $8_e + 4_b$, are the same and are shown in Fig. 5. It can be seen that no value of θ_b gives the required oxygen contributions, and therefore these

Table V.

reflection	Oxygen phase contribution to amplitude of reflection required at $Sb\theta_b = 46.2°$
0.26.0	(−)
0.28.0	(−)
0.30.0	(−)
0.32.0	uncertain
0.34.0	(+)

combinations may be eliminated. The variation of oxygen amplitude contribution with θ_b is the same for combinations (11), $8_e + 4_c$, and (12) $8_e + 4_d$, which are shown in Fig. 6. Both of these combinations give an excellent agreement with the required contributions for the $\theta_b = 22°$, $y = .06_1$, (this is the parameter of the 8 oxygen atoms in the general position, the other 4 oxygens being on one of the two possible rotation axes, 4_c of 4_d. The decision between these is arrived at in the determination of the x parameters of the oxygen atoms, where the more general reflections, $hk0$, are studied.)

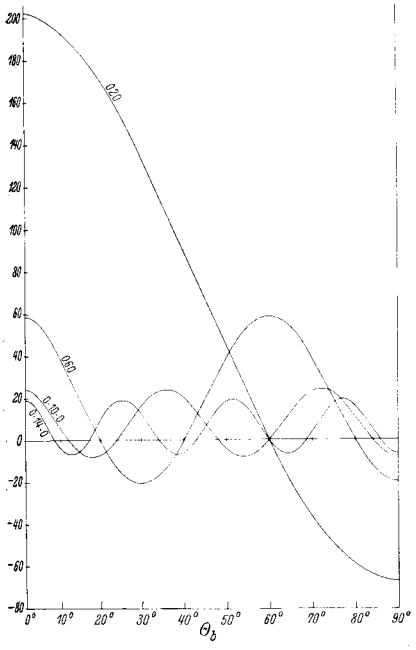

Fig. 5. Variations of oxygen amplitude contributions to orders of 010 (Cu-K_α radiation) with oxygen parameter, θ_b, for equipoint combinations $8_e + 4_a$ and $8_e + 4_b$.

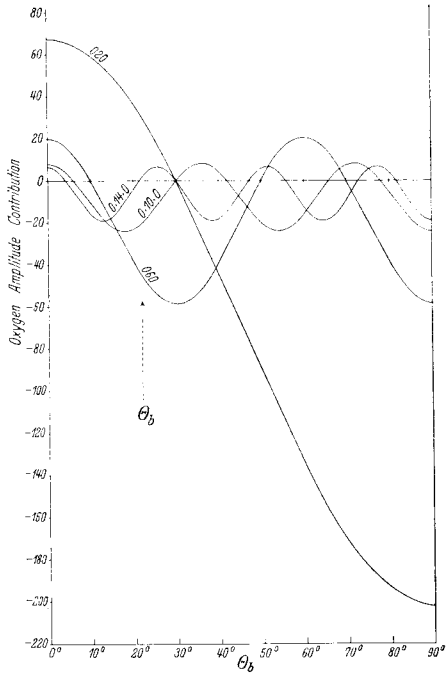

Fig. 6. Variations of oxygen amplitude contributions to orders of 010 (Cu-K_α radiation) with oxygen parameter, θ_b, for equipoint combinations $8_e + 4_c$ and $8_e + 4_d$.

The above discussion applies, as already noted, to reflections present on photographs taken with copper radiation. This solution of the oxygen y parameter may be confirmed by a study of the more sensitive $0k0$ reflections of great order present on photographs taken with molybdenum radiation. The oxygen phase requirements to give the observed intensity order, $24 > 28 > 32 \gg 26 > 30 \approx 34$, are given in

Table V. These conditions are simultaneously satisfied in a narrow region centering about $\theta_b = 20°$, $y = .056$, Fig. 7.

Determination of oxygen x parameter. The oxygen and antimony y parameters are now both accurately fixed, and the antimony x parameter is rather closely known. The reflections $hk0$ are therefore defined except for the uncertainty of the oxygen x parameter, which may accordingly be sought. The correct parameter will reproduce observed intensity relations among the $hk0$ spectra. The intensity calculations for $hk0$ take the following form:

h even, k even	h odd, k odd
$\sqrt{\frac{1+\cos^2 2\theta}{2\sin 2\theta}}\{8F_{Sb}\cos h\theta_a \cos(k\cdot 46\cdot 2^0) + 8F_0 \cos h\theta_a \cos(k\cdot 21^0) + 4F_0 \cos\left(h\begin{Bmatrix}90\\270\end{Bmatrix}\right)\cos(k\cdot 90^0)\}$	$-\sqrt{\frac{1+\cos^2 2\theta}{2\sin 2\theta}}\{8F_{Sb}\sin h\theta \sin(k\cdot 46\cdot 2^0) + 8F_0 \sin h\theta \sin(k\cdot 21^0) + 4F_0 \sin\left(h\begin{Bmatrix}90\\270\end{Bmatrix}\right)\sin(k\cdot 90$

The antimony θ_a parameter is purposely left in undetermined form; it will appear that if the general region of the antimony x parameter is known, the x parameter of oxygen can be fixed independently of it.

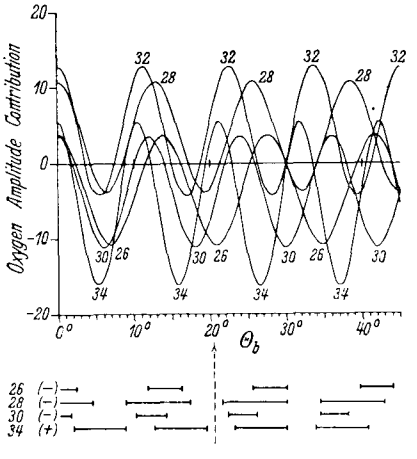

Fig. 7. Variations of oxygen amplitude contributions to some of the higher orders of 010 (*Mo*-K_α radiation) with oxygen parameter, θ_b, for equipoint combinations $8_e + 4_a$ and $8_e + 4_d$. The phase requirements of these contributions given in the text eliminate all but two small parameter regions, one of which (indicated by arrow) corresponds with the parameter derived in Fig. 6.

In the foregoing section, it was shown that the fourfold oxygen must be on either of the two possible rotation axes 4_c or 4_d located at either 90° and 270° respectively. This is allowed for by an alternative in the last term of the above calculation forms. One of these two alternatives may now be definitely eliminated: The reflection, 150, has an exceptionally high oxygen variation due to its small sin θ value (See Fig. 8). The absolute value of this reflection is zero on molybdenum radiation films (although it appears very faintly on copper radiation photographs). Fig. 8 shows that the value zero can only be attained by nearly a maximum negative total oxygen contribution to the amplitude of this reflection.

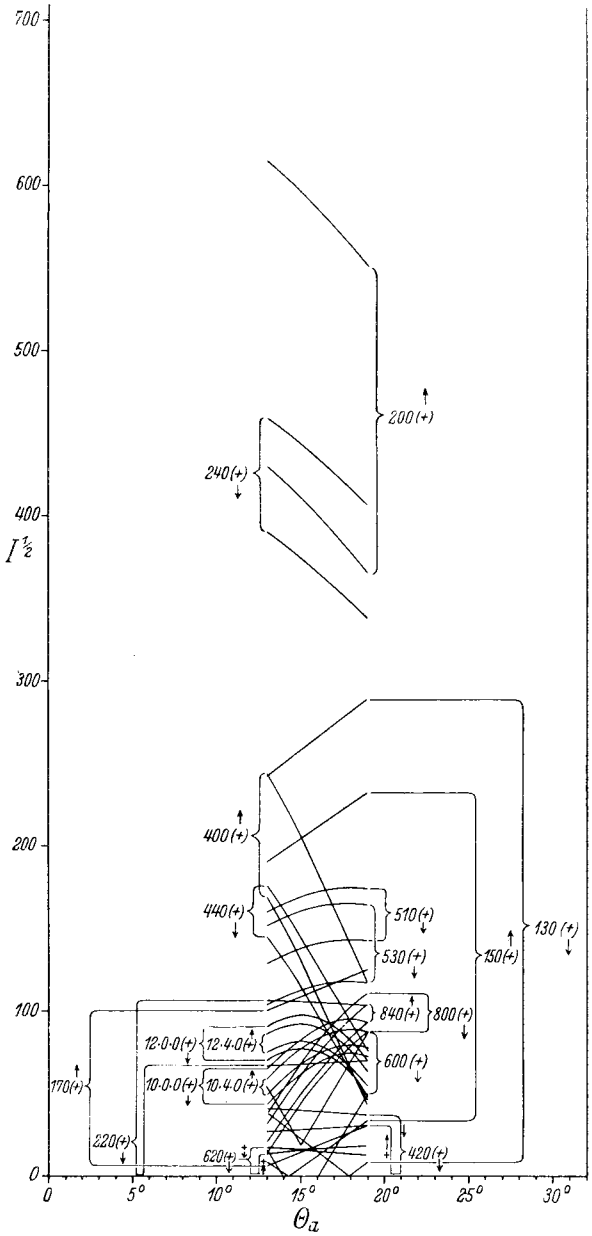

Fig. 8. Variations of intensity of some $hk0$ reflections (Mo-K_α radiation) with the antimony parameter θ_a. The widths of the bands represent the intensity variations possible with variations in oxygen positions. The direction of change of intensity for a positive oxygen contribution is indicated for each intensity band.

If the 4-fold oxygens are on the 270° equipoint, $4d$, then their individual amplitude contribution is positive, and the minimum possible net intensity of 150 would be a little less than that of 800, which is of intermediate intensity. Since the reflection 150 is substantially absent this eliminates equipoint $4d$ for the 4-fold oxygens, and determines the oxygen equipoint combination as $8_e + 4_c$, i. e., the oxygens are in the general positions and on the rotation axes through $[\![\frac{1}{4}\ \frac{1}{4}\ 0]\!]$.

The necessary oxygen amplitude contributions for the several reflections $hk0$ may be determined from a study of Fig. 8 together with the c-axis Weissenberg photograph made with molybdenum radiation. The conditions and the requirements they impose upon the oxygen contributions are given in table VI. The variation of the oxygen amplitude contributions of a number of the important reflections with the variation of the 8-fold oxygen parameter, x, is shown in Fig. 9. Study of Fig. 9 for the conditions listed in Table VI shows that they are satisfied at the unique parameter, $\theta_a = 53°$, $x = +.147$. A change in this parameter by $\theta = 5°$, $x = .014$, completely spoils the intensity relation (10.0.0 $>$ 10.4.0) $>$ (840 $>$ 800) $>$ (12.4.0 $>$ 12.0.0) so the parameter $x = .147$ may be considered accurate to about $\pm$ .007.

With the correct oxygen equipoint combination known, and the 8-fold oxygen x parameter accurately determined, the oxygen uncertainty in the determination of the antimony x parameter is removed. The net oxygen contributions at oxygen $x = +.147$ may be found from Fig. 9 to be as fol-

Table VI.

Intensity Contribution	Oxygen amplitude contribution requirement
$130 > \left\{\begin{matrix}8.00\\10.00\\12.00\end{matrix}\right\}$	130 cannot be (+) max.
150 absent	150 extremely (−)
$170 \approx 800$	170 nearly neutral
$200 \ll 240$	200 must be (−)
220 absent	220 must be very close to + 20
$400 \ll 440$	400 must be (−)
$420 > 600$ (absent)	420 must be extreme, preferably (−)
$620 > 600$ (absent)	$\left\{\begin{matrix}600 \text{ must be } (+)\\620 \text{ must be extreme, preferably } (+) \text{ max.}\end{matrix}\right.$
(10.0.0 > 10.4.0) > (840 > 800) > (12.4.0 > 12.0.0)	−(10.4.0 + 10.0.0) > (800 + 840) > (12.0.0 + 12.4.0)
$(510 > 530) > \left\{\begin{matrix}(840 > 800)\\(10.0.0 > 10.4.0)\\(12.4.0 > 12.0.0)\end{matrix}\right.$	$(530 - 510) > \left\{\begin{matrix}(800 + 840)\\(10.4.0 + 10.0.0)\\(12.0.0 + 12.4.0)\end{matrix}\right.$

lows for $h00$ reflections used in the determination of the antimony x parameter (see the original antimony x parameter determination, Fig. 1):

reflection	net oxygen amplitude contribution at oxygen $x=.147$
200	— 49
400	— 9
600	+ 3
800	+ $8\frac{1}{2}$
10.0.0	— 11
12.0.0	+ $4\frac{1}{2}$

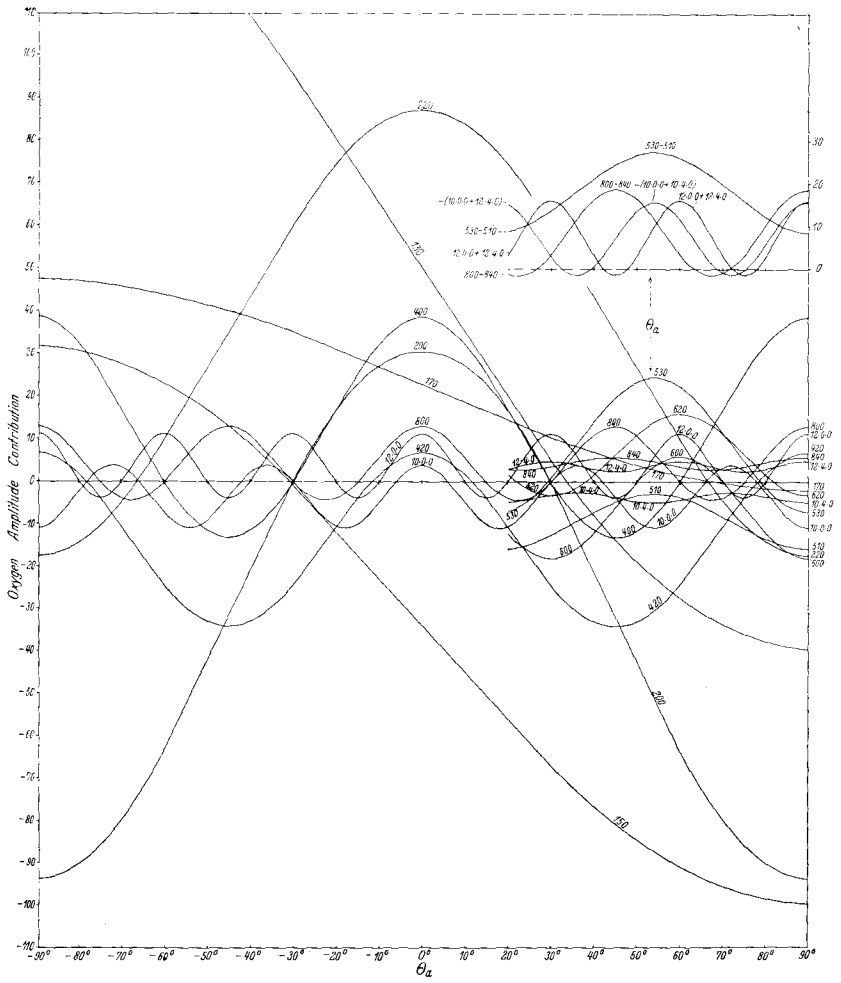

Fig. 9. Variations of oxygen amplitude contributions to the $hk0$ reflections (Mo-K_α radiation) appearing in Fig. 8, as functions of the oxygen parameter, θ_α, for the equipoint combination $8_e + 4_c$.

The critical region of Fig. 1 replotted with these oxygen phase allowances then permit a refining of the antimony x parameter to $\theta_a = 16° \pm 1°$ or $x = .444 \pm .003$.

Physically likely oxygen z and u parameters. The correct equipoint combination is now known, and the x and y parameters of all the atoms are unequivocally and accurately determined purely with aid of intensity criteria. The projection of the valentinite structure on (001) is therefore unequivocally and accurately determined. It is illustrated diagrammatically in Fig. 10. The only parameter normal to this projection known at this stage of the investigation is the antimony

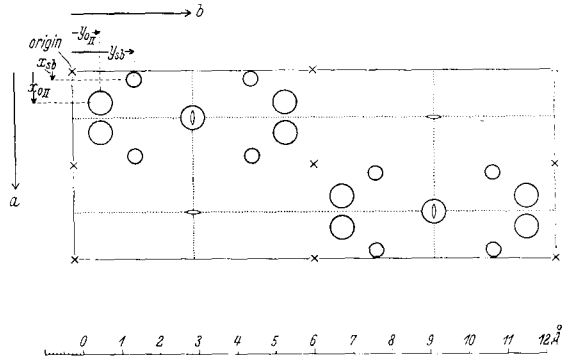

Fig. 10. Projection of the valentinite structure on (001). The small circles represent antimony atoms, the large circles oxygen atoms. The unit cell is outlined in fine full lines; (100) and (010) glide planes with glide component $c/2$ are indicated by dotted lines; symmetry centers on levels 0 and $\frac{1}{2}$ appear as crosses; the two kinds of 2-fold rotation axes, one of which is occupied by O_I atoms, are indicated by conventional symbols.

parameter, $\theta_c = 63\frac{1}{2}° \pm 2\frac{1}{2}°$, $z = .1764 \pm .0069$. A study of the projection together with this antimony parameter shows that the only physically acceptable interpretation of these data is that the 8-fold oxygen atoms are between pairs of antimony atoms (between (100) glide equivalents), and form chains with these extending down the c axis. Since the antimony positions are known, the oxygen elevations are fixed if the oxygen atoms are to occur equally spaced between antimony atoms, the only reasonable physical interpretation. If this is the case, the 8-fold oxygen atoms have a z parameter of either .0065 or $-.1418$. Now, this 8-fold oxygen is in the immediate region of a symmetry center, so that a centrosymmetrically equivalent oxygen atom is nearby. These are separated by about 2.04 Å for the first possible parameter and 2.54 Å for the

second possible parameter. The first distance is closer than known oxygen-oxygen separations, while the second is approximately the standard separation. The 8-fold oxygen parameter, $z = -.1418$ may therefore be accepted as the physically likely one.

Complete sets of antimony and 8-fold oxygen parameters are now available. They define an antimony-oxygen distance of 2.00 Å, which is in good agreement with the electron-pair bond radius sum, 2.02 Å. If this antimony-oxygen separation continues to hold for the distance between the antimony atoms and the 4-fold oxygens, then the latter must have a u parameter of either $-.174$ or .026. In the former case, the 4-fold and 8-fold oxygens occur on almost exactly the same vertical levels and have a spacing of about 2.46 Å; in the latter case they occur spaced almost exactly halfway between one another and have a spacing of about 2.61 Å. The first possible parameter gives too close an oxygen-oxygen separation without any obvious physical or chemical justification for it, consequently the second parameter, $u = .026$, may be accepted as the more likely one.

It should be stated at this point that the oxygen parameters, z and u, suggested by the above physical discussion, are tied directly to the antimony z parameters by dimensional considerations. The space group symmetry is such that if this antimony z parameter is increased, the oxygen parameters above mentioned are increased by the same amount, Δ, without in any other way changing the discussion. This leaves all interatomic distances mentioned the same, with the exception of the separation between the centrosymmetrical 8-fold oxygen atoms. For the antimony z parameter used, this gives an oxygen-oxygen distance of 2.54 Å, as already mentioned. The antimony z parameter limits have already been defined as $\pm .0069$. This allowance permits the centrosymmetrical oxygen separation to rise as large as 2.59 Å or fall as low as 2.50 Å.

The parameters of the valentinite structure at this point are as follows:

	x	y	z	u
Sb	.0444	.1283	$.176 \div \triangle$	
O_{I}				$.026 \div \triangle$
O_{II}	.1472	.058	$-.1418 + \triangle$	

Final Parameters.

To check the structure suggested by the physical requirements discussed in the last section, the intensities of a set of representative

reflections involving the z and u parameters were calculated. For this purpose the following $0kl$ reflections were used:

002	004	006	008	0.0.10	0.0.12	0.0.14
012	014	016	018			
022	024	026	028			
032	034	036	038			
042	044	046	048			
052	054	056				
062	064	066				
	074	076				
	084	086				

The $0k4$ and $0k6$ reflections were carried somewhat farther than the other reflections because some of them are quite sensitive to the vertical parameters to be tested. The intensity order calculated with the parameters listed in the foregoing section was in comparatively satisfactory agreement with the observed intensity order, but there is a very distinct improvement made by adding a small Δ correction as allowed for in the last section. A θ_c increase of $+1°$, equivalent to a parameter increase of $+ .002_8$, gives an excellent agreement between calculated and observed intensities for this group of $0kl$ reflections, as shown in Table VII.

Table VII. Calculated and observed intensities of important $0kl$ reflections. (Arrows indicate observed positions not corresponding with calculated order.)

reflection	$\sqrt{I}$ calculated	reflection	$\sqrt{I}$ calculated
002	370.3	036	62.8
012	340.4	062	48.2
042	330.6	076	47.8
052	313.8	056	47.0
054	230.7	0.0.12	43.5
014	217.1	018	41.5
032	207.7	084	33.8
034	198.7	024	31.5
006	188.3	022	28.4
046	163.3	038	24.6
074	141.4	0.0.10	17.9
086	140.6	066	13.4
048	117.7	028	10.1
008	112.9	026	5.3
0.0.14	91.7	064	1.5
004	86.6		
044	83.2		
016	80.0		

Three inconsequential discrepancies remain: The relatively lower visually estimated intensity of 0.0.14 is obviously due to the fact that it is resolved into an $\alpha_1 + \alpha_2$ doublet. (This is the case also for 0.0.10 (absent) and 0.0.12 (very weak), but these reflections are already so weak that the further weakening due to resolution into doublets makes very little difference.) The only other discrepancies in observed intensity order are possibly slightly high calculated positions of 062 and 084, as indicated. With the three exceptions noted, the observed and calculated intensity orders are in perfect agreement.

The final parameters, with due account given to the Δ correction, are as follows:

	x	y	z	u
$8Sb$	$.044_4$	$.128_3$	.179	
O_{I}				.029
O_{II}	.147	.058	.139	

Remarks on the Valentinite Structure.

A photograph of a model[1]) of the valentinite structure is shown in Fig. 11. Data for the construction of such a model are listed in Table VIII.

The valentinite structure is composed of indefinitely long molecules:

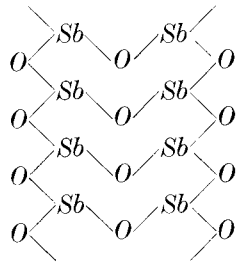

extending in the direction of the c axis and located on one of the two sets of 2-fold axes of the space group D_{2h}^{10}. The smallest Sb-O distances (Table IX) within molecules are all 2.00 Å, which correspond well with the tetrahedral Sb-O electron-pair bond radius sum[2]), 2.02 Å. (It is somewhat less than the "normal-valence" radius sum[3]), 2.07 Å.) That

1) Buerger, M. J., and Butler, Robert D., A technique for the construction of models illustrating the arrangement and packing of atoms in crystals, Amer. Min. **21** (1936) 150.

2) Pauling, Linus, and Huggins, M. L., Covalent radii of atoms and interatomic distances in crystals containing electron-pair bonds, Z. Kristallogr. (A) **87** (1934) 218.

3) Pauling, Linus, and Huggins, M. L., op. cit. p. 224.

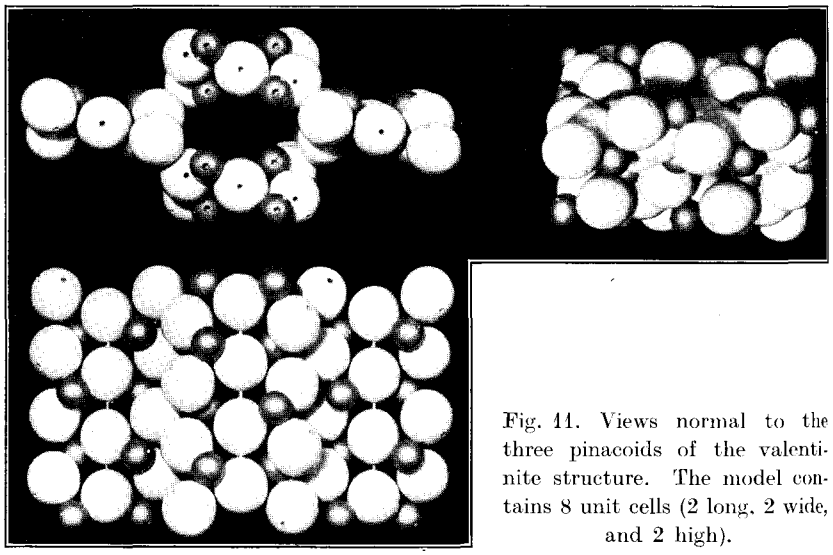

Fig. 11. Views normal to the three pinacoids of the valentinite structure. The model contains 8 unit cells (2 long, 2 wide, and 2 high).

Table VIII.

Data for the construction of a packing model of valentinite.

Ball designation	Ball diameter	Number of balls required for 4 unit cell model as illustrated in Fig. 11	Drilling co-ordinates of pinning holes		Pin joins ball to
			ϱ	q	
Sb_R	$\frac{3}{4}''$	16	$114\frac{3}{4}$	0	O_{I}
			$149\frac{3}{4}$	244	$O_{\mathrm{II}R}$
			$60\frac{1}{2}$	$273\frac{1}{2}$	$O_{\mathrm{II}L}$
Sb_L	$\frac{3}{4}''$	16	$114\frac{3}{4}$	0	O_{I}
			$149\frac{3}{4}$	116	$O_{\mathrm{II}L}$
			$60\frac{1}{2}$	$86\frac{1}{2}$	$O_{\mathrm{II}R}$
O_{I}	$1\frac{1}{4}''$	16	$65\frac{1}{4}$	0, 180	Sb_R or Sb_L
			180	0	O_{I}
			0	0	O_{I}
$O_{\mathrm{II}R}$	$1\frac{1}{4}''$	16	$30\frac{1}{4}$	0	Sb_R
			$55\frac{1}{2}$	105	$O_{\mathrm{II}L}$
			$119\frac{1}{2}$	270	Sb_L
$O_{\mathrm{II}L}$	$1\frac{1}{4}''$	16	$30\frac{1}{4}$	0	Sb_L
			$55\frac{1}{2}$	255	$O_{\mathrm{II}R}$
			$119\frac{1}{2}$	90	Sb_R

Table IX.

Important interatomic distances in valentinite.

atom	co-ordinates	neighbor	co-ordinates	distance
Sb	xyz	*Sb*	$\frac{1}{2}-x,\ y,\ \frac{1}{2}+z$	3.38 Å
		Sb	$\frac{1}{2}-x,\ \frac{1}{2}-y,\ z$	3.65
		Sb	$x,\ \frac{1}{2}-y,\ \frac{1}{2}+z$	4.07
		O_{I}	$\frac{1}{4},\ \frac{1}{4},\ u$	2.00
		O_{I}	$\frac{1}{4},\ \frac{1}{4},\ \frac{1}{2}+u$	2.63
		O_{II}	$x,\ y,\ z$	2.00
		O_{II}	$\frac{1}{2}-x,\ y,\ \frac{1}{2}+z$	3.05
		*O_{II}	$\bar{x},\ \bar{y},\ \bar{z}$	2.51
O_{I}	$\frac{1}{4}\frac{1}{4}u$	*Sb*	$x,\ y,\ z$	2.00
		Sb	$\frac{1}{2}-x,\ y,\ \frac{1}{2}+z$	2.63
		O_{I}	$\frac{1}{4},\ \frac{1}{4},\ \frac{1}{2}+u$	2.71
		O_{II}	$x,\ y,\ z$	2.61
		O_{II}	$\frac{1}{2}-x,\ y,\ \frac{1}{2}+z$	3.04
O_{II}	xyz	*Sb*	$x,\ y,\ z$	2.00
		Sb	$\frac{1}{2}-x,\ y,\ \frac{1}{2}+z$	3.05
		Sb	$-x,\ -y,\ -z$	2.51
		O_{I}	$\frac{1}{4},\ \frac{1}{4},\ u$	2.61
		O_{I}	$\frac{1}{4},\ \frac{1}{4},\ \frac{1}{2}+u$	3.04
		O_{II}	$\frac{1}{2}-x,\ y,\ \frac{1}{2}+z$	2.89
		*O_{II}	$\bar{x},\ \bar{y},\ \bar{z}$	2.54

Note: All interatomic distances are to atoms in the same $(Sb_2O_3)_\infty$ chain molecule except those indicated by an asterisk, thus: *

the observed distance is slightly less than the tetrahedral *Sb-O* radius sum might be expected because only three of the four possible tetrahedral positions are filled in *Sb* and only two in *O*. This decrease in co-ordination might easily lead to the smaller observed *Sb-O* separation as compared with that calculated for full tetrahedral co-ordination. That the antimony oxygen-bonding is really of a directed type is farther shown by the valence angles, Table X. The O_{I} valence angles are ca. 132°, the O_{II} valence angles are about 116°. These values are similar to those found in other simple compounds containing oxygen, the variation being from about 100° to 130° where ring formation does not limit it. The antimony valence angles also have about the expected values.

Table X.

Valence Angles in Valentinite.

$O_{\mathrm{I}}-Sb-O_{\mathrm{II}}$	81°, 99°	$Sb-O_{\mathrm{I}}-Sb$	132°
$O_{\mathrm{II}}-Sb-O_{\mathrm{II}}$	93°	$Sb-O_{\mathrm{II}}-Sb$	116°

The $(Sb_2O_3)_\infty$ chain molecules pack together in the valentinite structure in such a way that a side oxygen atom of one $(Sb_2O_3)_\infty$ chain butts up against a centrosymmetrically equivalent oxygen atom in the neighboring chain. This constitutes the closest oxygen-oxygen approach (2.54 Å) in the structure. The vertical alignment of centrosymmetrical chain molecules is such that the above-mentioned side oxygen comes to a position just opposite an antimony atom in the neighboring chain. This *Sb-O* distance is 2.51 Å and it probably represents a weak, secondary *Sb-O* bond. Presumably it is this bond which is especially important in causing the chain molecules to hold together to form a crystal.

This structure accounts well for the very perfect valentinite {110} cleavage. In breaking the crystal, the weaker intermolecular bonds should give way first, and these are found only in planes in the zone [001]. In this zone the bonds are most sparsely distributed along {110}, which is actually the best cleavage, and next most sparsely along {010}, which is actually the next best cleavage.

Standard references differ with regard to the relative perfections of the several valentinite cleavages and even with regard to the presence or absence of them. We have been unable to check the relative perfections of cleavages indicated in the following references:

Authority	Prismatic cleavage	Pinacoidal cleavage
Groth[1])	very perfect	very perfect
Hintze[2])	perfect	perfect
Dana[3])	perfect	perfect
Winchell[4])		perfect
Larsen and Berman[5])		perfect

In our experience, the cleavage is somewhat different in sublimed, chemically pure material and in the natural mineral. In the sublimed material, the prismatic is so perfect that the pinacoidal cleavage is difficult to develop at all. In the natural mineral valentinite, the pinacoidal becomes detectable, but always remains, at best, imperfect, and

1) Groth, P., Chemische Kristallographie, part. 1. Leipzig 1906, 109.

2) Hintze, Carl, Handbuch der Mineralogie. Bd. 1, Abt. 2. Leipzig 1915, 1238.

3) Dana, Edward Salisbury, The system of Mineralogy, sixth edition. New York 1914, 200.

4) Winchell, Alexander N., Elements of optical mineralogy, Part II, 2nd edition, New York 1927, 45.

5) Larsen, Esper S., and Berman, Harry, The microscopic determination of the nonopaque minerals (second edition) U. S. Geolog. Surv. Bull. 848 (1934) 211.

the discrepancy may lie in the composition of the material used by Bozorth in establishing the senarmontite parameters. He used senarmontite from Mt. Hamimet, Algeria, for which he records impurities to the extent of 3% arsenic, 10% alkaline earths, and a trace of bismuth. It is recognized also that interatomic distances need not be the same in polymorphic forms. It would be interesting to redetermine the parameters on senarmontite made by subliming chemically pure antimonous oxide below the transition temperature in an inert atmosphere.

We are indebted to Mr. Richard Hanau for preparing tracings of the original working drawings.

Received 30 June 1937.